Published online 30 September 2016 *Nucleic Acids Research, 2017, Vol. 45, No. 1* **215–230**
doi: 10.1093/nar/gkw882

Esc2 promotes Mus81 complex-activity via its SUMO-like and DNA binding domains

Marek Sebesta[1,2,3], Madhusoodanan Urulangodi[3], Barbora Stefanovie[1,2,4,†], Barnabas Szakal[3,†], Martin Pacesa[1], Michael Lisby[5], Dana Branzei[3] and Lumir Krejci[1,2,4,*]

[1]National Centre for Biomolecular Research, Masaryk University, Kamenice 5/A4, CZ-62500 Brno, Czech Republic, [2]Department of Biology, Masaryk University, Kamenice 5/A7, CZ-62500 Brno, Czech Republic, [3]IFOM, the FIRC Institute of Molecular Oncology, Via Adamello 16, IT-20139 Milan, Italy, [4]International Clinical Research Center, Center for Biomolecular and Cellular Engineering, St. Anne's University Hospital Brno, Pekarska 53, CZ-656 91 Brno, Czech Republic and [5]Department of Biology, University of Copenhagen, DK-2200 Copenhagen, Denmark

Received May 15, 2016; Revised August 30, 2016; Accepted September 22, 2016

ABSTRACT

Replication across damaged DNA templates is accompanied by transient formation of sister chromatid junctions (SCJs). Cells lacking Esc2, an adaptor protein containing no known enzymatic domains, are defective in the metabolism of these SCJs. However, how Esc2 is involved in the metabolism of SCJs remains elusive. Here we show interaction between Esc2 and a structure-specific endonuclease Mus81-Mms4 (the Mus81 complex), their involvement in the metabolism of SCJs, and the effects Esc2 has on the enzymatic activity of the Mus81 complex. We found that Esc2 specifically interacts with the Mus81 complex via its SUMO-like domains, stimulates enzymatic activity of the Mus81 complex *in vitro*, and is involved in the Mus81 complex-dependent resolution of SCJs *in vivo*. Collectively, our data point to the possibility that the involvement of Esc2 in the metabolism of SCJs is, in part, via modulation of the activity of the Mus81 complex.

INTRODUCTION

Replication of damaged DNA leads to replication fork stalling and accumulation of DNA gaps that may result in genome instability. Such instability was implicated in increased mutagenesis, in gross chromosomal rearrangements (GCR), and is thought to be the driving force for carcinogenesis (1). DNA damage tolerance (DDT) mechanisms are crucial to promote replication completion by mediating fork restart and filling of DNA gaps (2,3). Genetic studies have delineated two main pathways of DDT: error-free damage-bypass via recombination mechanisms and translesional synthesis (TLS)-mediated bypass, also called error-prone DDT. Error-free DDT involves template switching (TS) from the damaged parental DNA to the undamaged, newly synthesized sister chromatid, and proceeds via the transient formation of sister chromatid junction (SCJ) intermediates. In this process, Rad18/Rad5-dependent polyubiquitylation of PCNA acts in conjunction with a subset of homologous recombination factors to mediate SCJ formation in S-phase (4–8). In addition, later in the cell cycle, another recombination pathway, suppressed early in S phase, can be used to repair persistent DNA damage (5,8). The Sgs1 helicase, together with Top3 and Rmi1 (henceforth, the STR-complex; BTR-complex in humans), functions downstream of PCNA polyubiquitilation in error-free DDT by processing the damage-bypass SCJs to yield preferentially non-crossover recombination intermediates (5,8,9).

Recent work has shown that Mus81-Mms4 nuclease complex (henceforth termed the Mus81 complex) serves to back up the STR complex in resolving SCJs that persist in G2/M (9,10). However, deletion of either member of the Mus81 complex leads to no discernible accumulation of SCJ in S-phase, suggesting that the Mus81 complex plays a limited role in SCJs resolution (9,10). The Mus81 complex is a structure-specific endonuclease, which *in vitro* cleaves a diverse array of complex DNA structures, such as 3′ flap, fork, (nicked) Holliday and D-loop structures, some of which also arise during error-free DDT (11–15). Based on the sensitivity of *mus81Δ* cells to DNA damaging agents inducing fork stalling (hydroxyurea (HU), campthotecin (CPT)), it was also proposed that the Mus81 complex cleaves stalled/collapsed replication forks to promote fork-restart (16–18). Additionally, activity of the Mus81 complex may promote genome stability during S-phase by re-

*To whom correspondence should be addressed. Tel: +420 549493767; Fax: +420 549492556; Email: lkrejci@chemi.muni.cz
†These authors contributed equally to the work.
Present addresses:
Marek Sebesta, Sir William Dunn School of Pathology, University of Oxford, South Parks Road, Oxford OX1 3RE, UK.
Martin Pacesa, Institute of Molecular Life Sciences, University of Zurich, Winterthurerstrasse 190, CH-8057 Zurich, Switzerland.

solving collisions between D-loop structures, emanating from error-free DDT, and replication forks (19). In the later stages of recombination-mediated DDT, as well as during canonical recombination-mediated double strand break (DSB) repair, the Mus81 complex can resolve recombination intermediates, forming both cross-over (CO) and non-crossover (NCO) products (9,20,21). Additionally, human MUS81 complex promotes replication completion at common fragile sites after the bulk of DNA replication has been completed, being required for initiation of mitotic DNA synthesis (22–24). The activity of the Mus81 complex is regulated by phosphorylation of the Mms4 subunit with various outcomes, depending on the cell cycle stage and the kinase involved. During S-phase, the activity of Mus81–Mms4 is counteracted by DNA damage checkpoint kinases (9), while in G2/M phase, CDK-dependent phosphorylation of Mms4 (25,26) promotes HJ resolution by the Mus81 complex (9,27). This intricate network of phosphorylation events play a crucial role in ensuring genome stability by reducing CO formation emanating from the error-free DDT pathway that accompanies replication.

Establishment of silent chromatin 2 (*ESC2*) was first identified as a factor promoting gene silencing (28). Sequence analyses revealed that Esc2 belongs to a conserved, eukaryotic-specific *Sp*Rad60-*Sc*Esc2-*Hs*NIP45 (RENi) family (29). A feature of the members of the RENi family lies in their protein structure, which consists of a tandem of two SUMO-like domains (SLDs) (in case of Esc2, separated by a highly structured, helical domain) at their C-terminus, and a polar, unstructured N-terminal domain. Importantly, Esc2 plays a role in the error-free DDT pathway as evidenced by *esc2Δ* cells being sensitive to the DNA damaging agent methyl-methane sulphonate (MMS) and accumulating, in a manner reminiscent of STR-complex mutants, SCJs during replication of damaged templates (30,31). Our recent work uncovered a two-faceted role of Esc2 in recombination-mediated DDT. An early role, whereby Esc2 promotes recombination-mediated damage-bypass by limiting Rad51-dismantling by Srs2 (32) and a later role related to the metabolism of SCJs (30,31). However, the molecular mechanism by which Esc2 is involved in the metabolism of SCJs remains unknown.

In this study, we explored the possibility that Esc2 and the Mus81 complex may cooperate in resolution of recombination intermediates that arise during the error-free DDT pathway. We first determined that Esc2 preferentially binds Holliday structures *in vitro* through its N-terminal domain. Later, we established that Esc2 directly interacts with the Mus81 complex. This interaction can be detected throughout the cell cycle and requires the C-terminal SLD domains of Esc2. Furthermore, we tested the functional consequence of the interaction between Esc2 and the Mus81 complex, and found that Esc2 specifically stimulates the activity of the Mus81 complex on all tested substrates *in vitro* and collaborates with the Mus81 complex in the late resolution of SCJs in mitosis. Our data point to the possibility that one of the mechanisms by which Esc2 is involved in SCJ metabolism in mitosis is by recognizing the structures and promoting the activity of the Mus81 complex.

EXPERIMENTAL PROCEDURES

Yeast strains

Yeast strains were constructed as described in (9,33). Yeast strains used in this study are listed in the Supplementary Table S1.

Plasmids and DNA substrates

To express and purify Esc2 from *E. coli* as a fusion with Gluthation-S-transferase (GST)-tag and a PreScission protease cleavage site between GST and Esc2, DNA fragment containing *ESC2* ORF was cloned into *Bam*HI and *Sal*I sites of expression vector pGEX6-P1, yielding plasmid pGEX6-P1-*ESC2*. Plasmids for purification of truncated forms of Esc2 ($Esc2^{1–199}$, $Esc2^{1–294}$ and $Esc2^{1–374}$) were generated by site-directed mutagenesis of the plasmid pGEX6-P1-*ESC2*, introducing a STOP codon at positions corresponding to amino-acids Y200, E295 and G375, respectively. To express and purify Esc2 fragments $Esc2^{193-456}$, $Esc2^{200-456}$ and $Esc2^{384-456}$ in fusion with GST-tag, DNA fragments containing the corresponding DNA sequences were cloned into *Eco*RI and *Sal*I sites of pGEX6-P1, yielding plasmids pGEX6-P1-$ESC2^{193–456}$, pGEX6-P1-$ESC2^{200–456}$ and pGEX6-P1-$ESC2^{384–456}$, respectively. Plasmids for purification of Esc2 fragments $Esc2^{193–294}$ and $Esc2^{193–374}$ were generated by site-directed mutagenesis of pGEX6-P1-$ESC2^{193–456}$, introducing a STOP codon at position corresponding to amino-acids E295 and G375, respectively. Primers used to generate various forms of Esc2 protein were purchased from VBC Biotech and are listed in Supplementary Table S2. The DNA substrates, used in the study, were prepared as described previously (34).

Purification of Esc2 and its truncations

The *ESC2* and its truncated forms were expressed as a GST fusion proteins in *E. coli* BL21 RIPL cells (induction: 30°C, 0.5 mM IPTG, 3 h). All purification steps were performed at 4°C. Ten grams of *E. coli* cell paste were sonicated in 50 ml of lysis buffer C (50 mM Tris–HCl, 10% sucrose (w/v), protease inhibitors (aprotinin, chymostatin, leupeptin, pepstatin A, benzamidine, each at 5 μg/ml), 10 mM EDTA, 1 mM dithiothreitol (DTT), 0.01% (v/v) Nonidet-P40, and 100 mM KCl; pH 7.5). The crude lysate was clarified by centrifugation (100 000 × g for 60 min). The supernatant was loaded onto a 10-ml Q sepharose column (GE Healthcare) equilibrated with buffer T (25 mM Tris–Cl, 10% (v/v) glycerol, 5 mM EDTA; pH 7.5) containing 100 mM KCl and eluted with a 150 ml linear gradient of 100–500 mM KCl in buffer T. The peak fractions were pooled and batched for 1 h with 2 ml of glutathione-sepharose 4B beads (GE Healthcare) equilibrated with buffer T containing 150 mM KCl. GST-Esc2 was eluted with 6 × 2 ml of 20 mM glutathione in buffer T containing 150 mM KCl. After the elution, fractions containing GST-Esc2 were pooled and split into two aliquots. The first aliquot was diluted with 5 ml of buffer T and loaded onto a 1-ml Mono Q column (GE Healthcare) equilibrated in buffer T containing 100 mM KCl. The GST-Esc2 fragments were eluted with a 20-ml

gradient of 100–600 mM KCl in buffer T. Fractions containing homogenous GST-Esc2 were concentrated in a Vivaspin concentrator (Sartorius Stedim Biotech), and stored in 10-μl aliquots at −80°C. The second aliquot was incubated with 5–25 μg of PreScission protease for 3 h at 4ºC, to cleave the GST-tag off. Next, the sample was diluted with 5 ml of buffer T and loaded onto a 1-ml Mono Q column (GE Healthcare) equilibrated in buffer T containing 100 mM KCl. Esc2 were eluted with a 20-ml gradient of 100–500 mM KCl in buffer T. Fractions containing homogenous Esc2 were concentrated in a Vivaspin concentrator (Sartorius Stedim Biotech) and stored in 10-μl aliquots at −80°C. GST-Esc2$^{193–294}$ and GST-Esc2$^{193–374}$ were expressed and purified as described above, with the exception that the initial Q-sepharose chromatographic step was omitted.

Purification of the Mus81 complex

The Mus81 complex was purified as described in (34), with the exception that *E. coli* Rossetta 2 pLysS was used as host strain for expression of the complex.

Co-immunoprecipitation

Four hundred ml of exponentially growing cells (1.2×10^7 cells/ml) were suspended in 4 ml of lysis buffer (50 mM K-HEPES pH 7.5, 140 mM NaCl, Triton X-100, 1 mM EDTA, 0.1% Na-deoxycholate) supplemented with Protease inhibitor cocktail (Roche, 1 tablet per 12.5 ml of lysis buffer), NEM (20 mM), IAA (100 μM), phosphatase inhibitor cocktail 2 and 3 (5 μl each) and disrupted by liquid nitrogen with pestle and mortar as previously described (30). To the supernatant, 50 μl Protein-G Sepharose resin (50% slurry in lysis buffer) was added and incubated at 4°C for 1 h to pre-clear the lysate. Cleared supernatant was then incubated with 50 μl of 50% Protein-G Sepharose resin and 1.5 μg of FLAG or PK antibody for 5–6 h at 4°C. After washing the beads three times with 1 ml of lysis buffer, bound proteins were eluted with SDS-PAGE sample buffer (35 μl). Protein samples were resolved by gradient gels (4-20%, Bio-Rad) and transferred to Amersham Protran 0.45 nitrocellulose membrane (G5678144, GE). The experiments were done twice in independent biological experiments.

In vitro pull-down

Purified GST-Esc2s (3 μg) were incubated with the Mus81 complex (3 μg) in 30 μl of buffer T (20 mM Tris–HCl, 100 mM KCl, 1 mM DTT, 0.5 mM EDTA, and 0.01% Nonidet P-40; pH 7.5) for 30 min at 4°C in the presence of GSH-beads. After washing the beads twice with 100 μl of buffer T, the bound proteins were eluted with 30 μl of 5% SDS. The supernatant (S), wash (W), and SDS eluate (E), 10 μl each, were subjected to SDS-PAGE analysis.

In vivo pull-down

GST or GST-fused proteins (5 μg) were immobilised on 30 μl of glutathione-sepharose 4B beads. Two hundred ml of (1.2×10^7 cells/ml) yeast cells were either arrested with α factor (for G1-phase of the cell cycle; 3 μg/ml), or released into media containing 200 mM HU from G1-arrest (for S-phase), or arrested with nocodazole (for G2/M; 10 μg/ml). Yeast native extract was prepared by lysis in liquid nitrogen (mortar and pestle) in 50 mM HEPES pH 7.4, 140 mM NaCl, 1 mM EDTA, 1% Triton X-100, 0.1% Na-deoxycholate, supplemented with protease inhibitor cocktail (Roche) and by pre-clearing by centrifugation. GST fusion proteins (5 μg), immobilised on GTH-beads, were incubated with 2.5 mg of yeast cell lysate at 4°C in the presence of inhibitor cocktail for 2–3 h. The beads were washed twice with Tris buffer (20 mM Tris–HCl, 150 mM NaCl, 1mM DTT, 1 mM EDTA, 10% glycerol, 0.1% Triton X-100; pH 7.5) and twice with Tris buffer containing 350 mM NaCl. The protein complexes, isolated on the beads, were subjected to a 10% SDS-PAGE and analysed by immunoblotting using antibodies recognising HA and PK epitope, respectively. The proteins were visualised by enhanced chemiluminescence (ECL), according to the manufacturer's instructions (SuperSignal West Dura, Thermo Scientific).

Live cell imaging

Cells were grown shaking in liquid synthetic complete medium supplemented with 100 μg/ml adenine (SC+Ade) medium at 25°C to OD600 = 0.2–0.3 and processed for fluorescence microscopy as described previously (35). For this study, the following fluorophores were used: yellow fluorescent protein (YFP, clone 10C) (36) and turquoise fluorescent protein (TFP) (37). Fluorophores were visualized on a Deltavision Elite microscope (Applied Precision, Inc) equipped with a 100× objective lens (Olympus U-PLAN S-APO, NA 1.4), a cooled Evolve 512 EMCCD camera (Photometrics, Japan), and an Insight solid-state illumination source (Applied Precision, Inc). Images were acquired using softWoRx (Applied Precision, Inc) software. Image analysis and fluorescence intensity quantification were done using Volocity software (PerkinElmer). Images were pseudo-coloured according to the approximate emission wavelength of the fluorophores.

Electrophoretic mobility-shift assay (EMSA)

Purified Esc2 and its truncated forms (16, 31, 63, 125, 250, 500 and 1000 nM) were incubated with the indicated fluorescently labeled substrate (7 nM) at 30°C in 10 μl of buffer D (40 mM Tris–HCl, 50 mM KCl, 1 mM dithiothreitol, 5 mM $MgCl_2$; pH 7.5) for 10 min. After addition of gel loading buffer (60% glycerol, 10 mM Tris–HCl, 60 mM EDTA, 0.10% Orange G; pH 7.4), the reaction mixtures were resolved in a 7.5% native polyacrylamide gels in 0.5xTBE buffer (45 mM Tris-borate, 1 mM EDTA; pH 7.5) at 4°C. The fluorescent DNA species were visualized and quantified using Fuji FLA 9000 imager with the Multi Gauge software (Fuji).

Nuclease assay

The nuclease assays with the Mus81 complex was performed essentially as described (34). Briefly, reaction mixtures containing the Mus81 complex (0.05 nM) and DNA substrate (7 nM) in 10 μl of buffer N (20 mM Tris, 100 mM KCl, 100 μg/ml bovine serum albumin, 0.2 mM DTT,

5% glycerol, and 10 mM $MgCl_2$; pH 8.0) were incubated at 37°C for 30 min in the absence or presence of Esc2 and its truncated forms (16, 31, 63, 125, 250, 500 and 1000 nM). After deproteinization by incubation with 0.1% SDS and 500 μg/ml of proteinase K at 37°C for 5 min, the reactions were mixed with 1/5 volume of loading buffer and resolved in a 10% polyacrylamide gel in 1× TBE buffer (90 mM Tris-borate, 2 mM EDTA; pH 7.5). The fluorescent DNA species were visualized and quantified as described above.

2D gel analysis and quantification of replication/ recombination intermediates

G2/M synchronized *sgs1* Tc-Esc2-AID (HY5351) and *sgs1* Tc-Mms4 (HY1946) cells were treated with MMS for 90 min (MMS), then released in YPD media in two identical sets of cultures. One set of *sgs1* Tc-Esc2-AID cultures was treated with tetracycline and auxin (Tc+Ax+), one set of *sgs1* Tc-Mms4 cultures was treated with tetracycline (Tc+), the other set remained untreated during the release. Samples were taken at the indicated time points for FACS, protein and 2D gel analysis. Replication intermediates were visualized using a radioactively labeled probe specific for *ARS305*. The quantification of replication intermediates was performed as described in (9). Mms4 and Esc2 (both tagged with HA) levels were analyzed by western blot, Pgk1 was used as a loading control. The experiments were performed twice with qualitatively identical results.

RESULTS

Esc2 preferentially binds Holliday junctions

Deletion of *ESC2* results in accumulation of unresolved SCJs upon replication of damaged template (30,31). However, based on bioinformatic analysis, Esc2 lacks any detectable domain that may be directly accountable for dissolution and/or resolution of these structures (29). Therefore, we first tested whether Esc2 binds to various DNA substrates *in vitro*. We incubated increasing concentrations of Esc2 with: (i) DNA substrates representing either simple ssDNA or dsDNA sequences; (ii) DNA structures that resemble replication intermediates (Y-form, 3′ flap, 5′ flap, and Fork); or (iii) DNA structures representing SCJs (nicked or intact Holliday junction structures (nHJ, HJ, respectively)). Using electrophoretic mobility-shift assay (EMSA) we assessed the DNA binding affinity of Esc2 (Figure 1A), where ∼30% of ssDNA and ∼50% of dsDNA was bound by 1 μM Esc2 (Figure 1B). Interestingly, it exhibited 4-fold higher affinity towards structures representing replication intermediates compared to ss or dsDNA. In particular, ∼50% of these intermediates were bound at 250 nM (Figure 1A, B). Even higher affinity was observed towards model SCJs (nHJ and HJ), binding ∼80% of the substrate at 125 nM (Figure 1A and B), representing additional 2-fold increase in affinity compared to the replication intermediates.

Next, we also examined the Esc2 domain responsible for DNA binding. To this end, we constructed a set of N-terminally, C-terminally, and internally truncated versions of Esc2. We first tested their folding by circular dichroism. Spectra of $Esc2^{200\text{-}456}$ and $Esc2^{\Delta 154\text{-}198}$ fragments were similar to the spectrum of wild type Esc2 protein, with prominent α-helices. $Esc2^{1–199}$ fragment showed a different type of spectrum, that resembles a poly-l-proline-II type (PPII) helix (Supplementary Figure S1B). Next, we determined affinity of the truncated versions towards HJs. As shown in Supplementary Figure S2, while Esc2 fragments $Esc2^{1–374}$, $Esc2^{1–294}$ and $Esc2^{1–199}$ bound HJs with similar affinities to the wild-type Esc2, the $Esc2^{1–151}$ did not bind DNA. Furthermore, N-terminally truncated version of Esc2 ($Esc2^{200–456}$) also did not bind HJ at concentrations up to 250 nM. At a very high concentration of $Esc2^{200–456}$ protein (1 μM), it bound 40% of HJ corresponding to a 16-fold decrease in affinity compared to the wild-type Esc2. To support the notion, that the DNA binding domain of Esc2 may be located on its N-terminus, we tested an internally truncated version of $Esc2^{\Delta 154–198}$, lacking AA154–198. It bound only ∼10% and 25% of the nHJ substrate at 250 nM and 1 μM, respectively, representing a 10-fold decrease in the affinity compared to wild-type protein (Supplementary Figures S2C and S8C). This data corroborates our earlier work concerning Esc2 binding to replication fork intermediates (32). In summary, Esc2 has very high affinity towards HJ and nHJ substrates and the region responsible for this binding is located within the region 154–198 of Esc2, providing a molecular rationale for its reported *in vivo* role of processing SCJs arising via DDT (32).

Esc2 interacts with the Mus81 complex regardless of the cell cycle stage or phosphorylation status of the Mms4 protein

The structure-specific Mus81 nuclease complex was recently implicated in the resolution of persistent SCJs arising during the error-free DDT specifically in G2/M (9,10). We asked if Esc2 affects Mus81-dependent resolution of SCJs and initially tested interaction between Esc2 and the Mus81 complex both *in vitro* and *in vivo*. Using *in vitro* pull-down assay we examined whether purified GST-tagged Esc2 is able to interact with the Mus81 complex. As shown in Figure 2A (lanes 5–7), GST-Esc2 efficiently interacted with the Mus81 complex, indicating direct physical interaction between Esc2 and the Mus81 complex.

Furthermore, we performed a series of *in vivo* pull-downs using cell extracts prepared from cells expressing HA-tagged Mms4 (Mms4-HA) (9) (Figure 2B). As detected by western-blot analysis of Mms4-HA using α-HA antibodies, GST-Esc2 (lane 3), in contrast to GST alone (lane 2), was able to pull-down the Mus81 complex (Figure 2B). Moreover, DNA does not mediate this interaction, as ethidium bromide (EtBr) did not interfere with the ability of GST-Esc2 to pull-down the Mus81 complex (Figure 2B, lane 4). To rule out the possibility that the tag present on Mms4 plays a role in the detected interaction between Esc2 and the Mus81 complex, we conducted the same experiment using cell extracts prepared from cells expressing C-terminally PK-tagged MMS4 (9). The same results as for Mms4-HA were observed (Supplementary Figure S3A), indicating that the tag present on Mms4 does not affect the interaction.

Next, we asked whether the interaction between Esc2 and the Mus81 complex is restricted to a particular stage of the cell cycle. To this end, we synchronized the cells expressing Mms4-HA at G1, G2/M and S phases of the cell cycle using α-factor, nocodazole and hydroxyurea (HU),

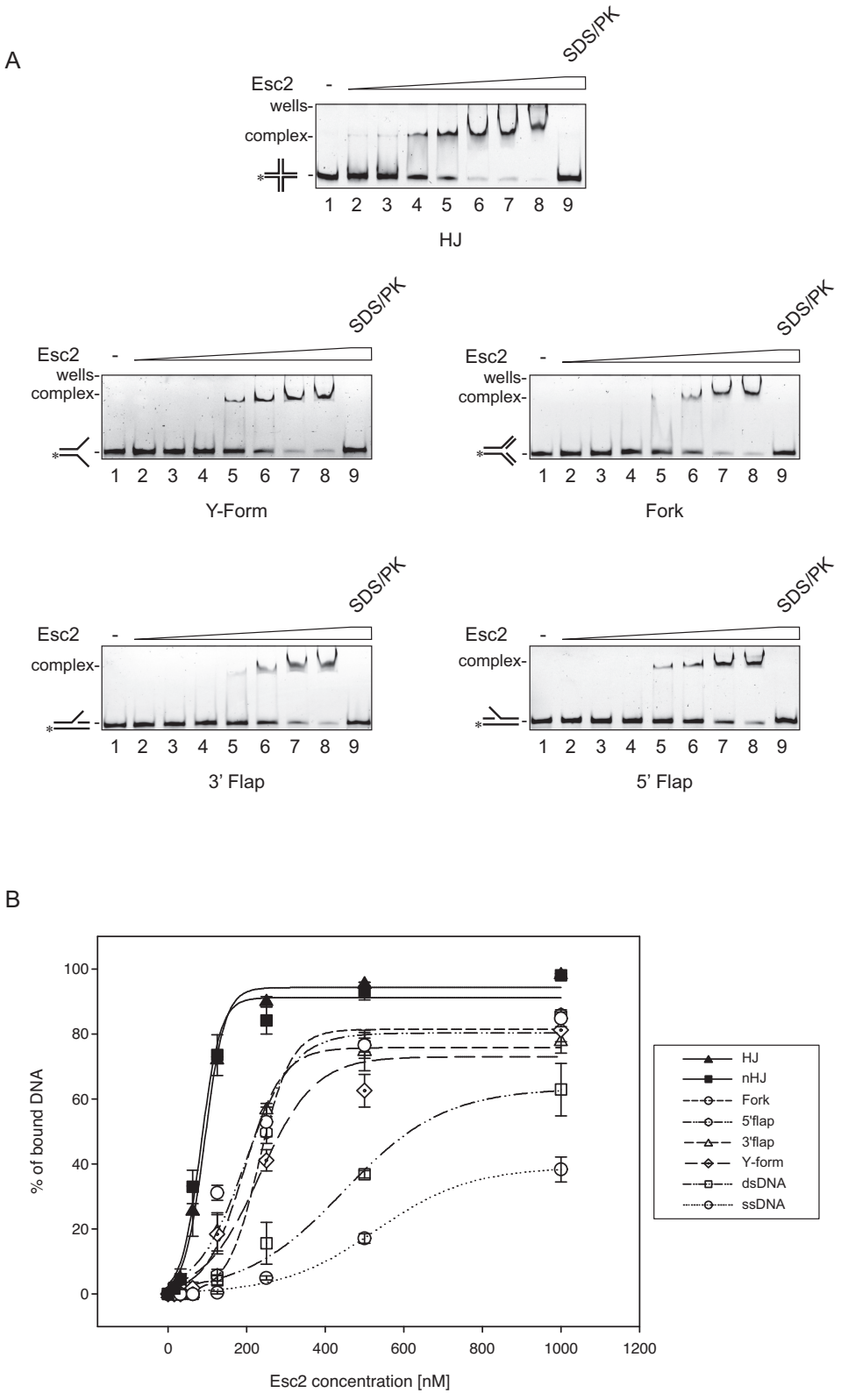

Figure 1. Esc2 preferentially binds Holliday junctions *in vitro*. (**A**) DNA binding properties of Esc2. Increasing concentrations of Esc2 (16, 31, 63, 125, 250, 500 and 1000 nM) were incubated with the indicated substrates (7 nM each). After incubation, the samples were separated on a native PAGE gel and analyzed. Lane 9 of the individual gels represents the control reaction treated with SDS/PK. (**B**) Quantification of the data shown in (A) as well as reactions with other DNA substrates not shown in the figure. Error bars represent standard error from three independent experiments. Where applicable, position of the wells is indicated.

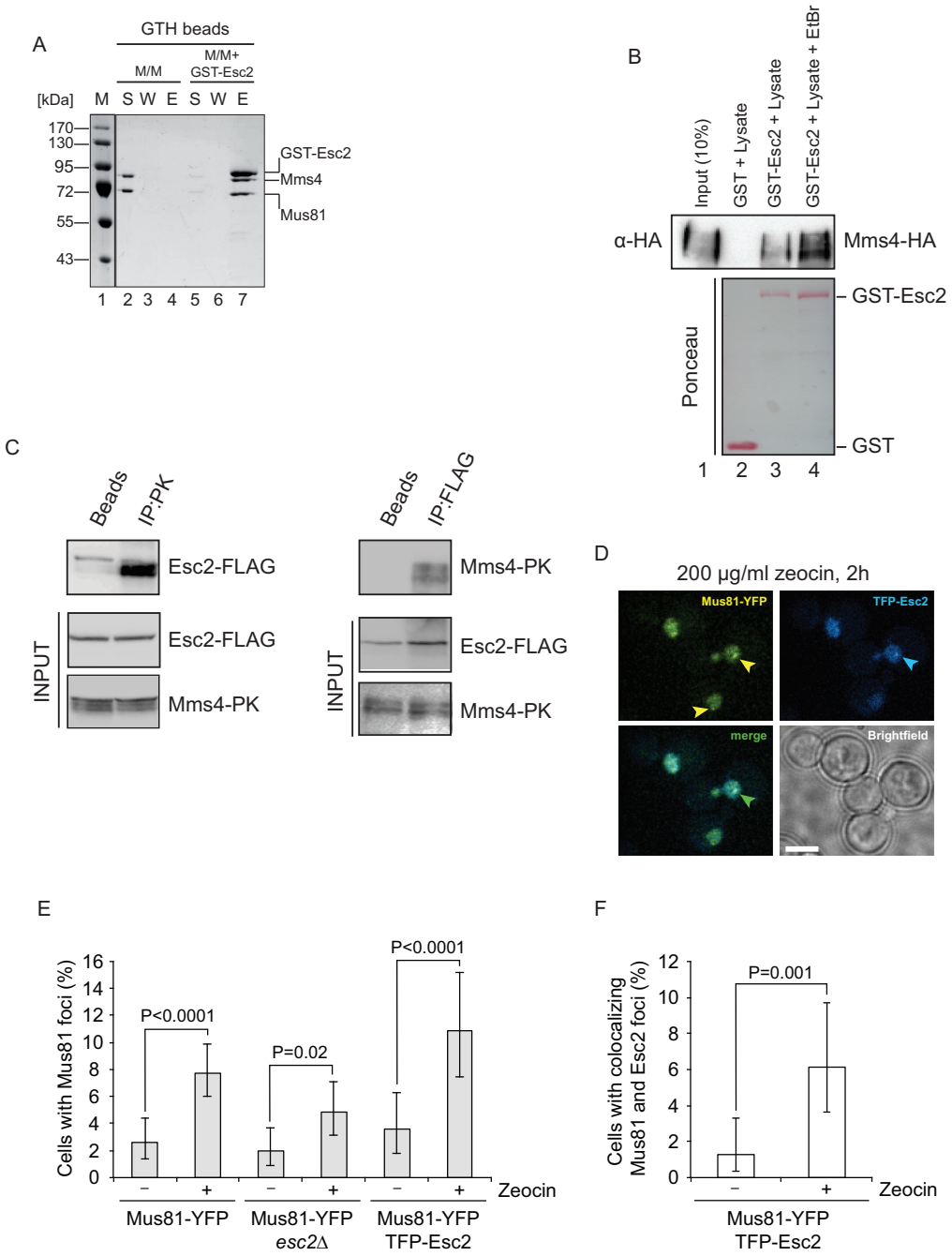

Figure 2. Esc2 interacts with the Mus81 complex. (**A**) Esc2 interacts with the Mus81 complex *in vitro*. Mus81/Mms4 complex (3 μg) was mixed with GST-Esc2 (3 μg) in the presence of glutathione beads (lanes 5–7). After incubation, the beads were washed and treated with SDS to elute bound proteins. The supernatants (S) with unbound proteins, the wash fraction (W), and the SDS elution (E) fractions were analyzed by SDS-PAGE and visualized by Coomassie Blue staining. Lanes 2–4 represent control experiment, where the Mus81 complex was incubated with glutathione beads alone. (**B**) The Mus81 complex interacts with Esc2 in an *in vivo* pull-down. Total cell lysates prepared from exponentially growing cells expressing Mms4-HA were incubated with GST or GST-Esc2. Following wash, the protein complexes were eluted and mixture subjected to 10% SDS-PAGE. Total cell lysates (10% input) and beads of corresponding pull-downs were analyzed by western blotting using anti-HA antibody. Lane 3 represents GST-Esc2 incubated with total cell lysate in presence of Ethidium Bromide. The amount of GST and GST-Esc2 protein used is shown by Ponceau staining. (**C**) The Mus81 complex interacts with Esc2 in co-immunoprecipitation assay. Protein extracts from cells expressing both Flag-tagged Esc2 and PK-tagged Mms4 were subjected to immunoprecipitation (IP) using either FLAG or α-PK antibody. Empty beads with the antibody conjugated, were used as a control. Protein levels in the extracts (10% of the input) are shown below the IPs. (**D**) Esc2 and the Mus81 complex co-localize upon DNA damage. Representative images of Mus81 and Esc2 colocalization in the nucleus are shown. Yellow arrowheads indicate Mus81-YFP foci, blue arrowheads indicate TFP-Esc2 foci and green arrowheads indicate colocalization between the two proteins. Scale bar represents 3 μm. (**E**) Quantitative analysis of Mus81 and Esc2 foci. Cells expressing Mus81-YFP and TFP-Esc2 were untreated or incubated with Zeocin (200 μg/ml) for 2 h and focus formation was analyzed. Error bars represent the 95% confidence intervals. Significant differences (*P*) observed between untreated and treated cells were determined using one-tailed Fisher's exact test ($n > 150$). (**F**) The frequency of colocalization between Mus81 and Esc2 foci was determined for the experiment in panel (E). Error bars represent the 95% confidence intervals. Significant differences (*P*) observed between untreated and treated cells were determined using one-tailed Fisher's exact test.

respectively, and tested the interaction between GST-Esc2 and the Mus81 complex. As shown in Supplementary Figure S3B, Esc2 pulled down Mus81 complex from all tested cell extracts, suggesting that Esc2 interacts with the Mus81 complex throughout the cell cycle. Since the nuclease complex is phosphorylated in G2/M phase by Cdc5-dependent phosphorylation of Mms4 on various residues, including the prominent serine 56, and the phosphorylation correlates with improved ability of the Mus81 complex to cleave HJ-like substrates (9,25,26), we also tested whether the Esc2-Mms4 interaction is regulated by the phosphorylation status of Mms4. Therefore, we performed the *in vivo* pull-down with cell extracts expressing phosphomimic-allele of *MMS4* (*mms4*^{S56E}-HA) (9). GST-Esc2 pulled-down Mus81-Mms4^{S56E} similarly to the wild-type complex (Supplementary Figure S3C, compare lanes 5 and 6), indicating that Cdc5-mediated phosphorylation of Mms4 does not critically influence interaction between Esc2 and the Mus81 complex.

To further corroborate on Esc2 interaction with the Mus81 complex *in vivo*, we tested the interaction *in vivo* using co-immunoprecipitation (CoIP) experiments. We tagged Esc2 and Mms4 with Flag- and PK-tag, respectively, and expressed the genes from their native promoters. In our experiments, Flag-tagged Esc2 precipitates the Mus81 complex, as evidence by detection of PK-tagged Mms4 subunit (Figure 2C). Moreover, when we performed the CoIP experiment by precipitating PK-MMS4, we observed Flag-tagged Esc2 in the eluate fraction (Figure 2C). Furthermore, we monitored Esc2 and Mus81 foci formation and colocalization in unchallenged cells and cells treated with zeocin, a drug that generates DNA damage that is repaired via homology-mediated DNA repair. We tagged Esc2 N-terminally with turquoise fluorescent protein (TFP-Esc2) and Mus81 with yellow fluorescent protein at the C-terminus (Mus81-YFP). In untreated cells, only a small fraction of Mus81 foci colocalized with Esc2 (Figure 2D and E), which, after treatment with zeocin, resulted in significant increase of Esc2 and Mus81 colocalization (67%; Figure 2E and F). However, deletion of *ESC2* does not significantly reduce the Mus81 foci (Figure 2E), suggesting that Esc2 is not required for Mus81 recruitment to sites of zeocin-generated DNA lesions.

In summary, Esc2 protein interacts directly with the Mus81 complex both *in vitro* as well as *in vivo*, and this interaction is largely independent of the cell cycle stage or Mms4 phosphorylation status.

Esc2 interacts with the Mus81 complex via its SUMO-like domains

Identification of the interaction between Esc2 and the Mus81 complex prompted us to map the Esc2 domain responsible for the interaction with the Mus81 complex, using a set of N-terminally or C-terminally truncated versions of GST-tagged Esc2. These truncations were constructed to allow us to assess the role of individual SUMO-like domains (SLDs), as well as of the polar N-terminal domain (Figure 3A) in the interaction. Using pull-downs, we observed that the fragment of GST-Esc2 lacking both SUMO-like domains (GST-Esc2$^{1–199}$), failed to interact with the Mus81 complex from a cell extract (Figure 3B). This result suggested that the SLDs mediate the interaction between Esc2 and the Mus81 complex. To further test this, we performed *in vitro* pull-down experiments with purified proteins. We found that GST-Esc2$^{1–374}$ (Esc2 fragment lacking the SLD2 domain), GST-Esc2$^{1–294}$ (Esc2 fragment lacking the SLD2 and the helical domain separating the SLDs) interacted the with the Mus81 complex, though to a lesser extent compared to full-length Esc2 (Figure 3C, compare lanes 14, 15, respectively, with lane 13), indicating that the SLD2 plays an important role in the interaction. Indeed, while GST-Esc2$^{1–199}$ (fragment lacking both SLDs) was not able to interact with the Mus81 complex (Figure 3C, lane 16), the N-terminally truncated GST-Esc2$^{200–456}$ pulled-down the Mus81 complex efficiently (Figure 3C, lane 17). Taken together, the results suggest that the SLDs, but not the N-terminal domain of Esc2, mediate the interaction with the Mus81 complex. In line with this result, we also detected interaction between Esc2$^{\Delta 154–198}$ and the Mus81 complex (Supplementary Figure S8A). To compare the relative contribution of the individual SLDs, we tested three additional fragments: GST-Esc2$^{193–294}$ (SLD1 domain), GST-Esc2$^{193–374}$ (SLD1 and the helical domain), and GST-Esc2$^{384-456}$ (SLD2 domain). As shown in Figure 3C (lanes 18–20), SLD1-containing polypeptides interact with the Mus81 complex very weakly, in contrast to the fragment containing SLD2 that showed strong interaction with the Mus81 complex, comparable to that of the GST-Esc2$^{200–456}$ fragment.

The observation that the SLDs of Esc2 mediate the interaction, and their sequence similarity with yeast SUMO protein (Supplementary Figure S4A and (29)), prompted us to test direct interaction between ySUMO and the Mus81 complex. As seen in Supplementary Figure S4B, while the GST-Esc2 and GST-Esc2$^{384–456}$ (GST-SLD2) interact with the Mus81 complex, ySUMO has only very weak affinity towards the Mus81 complex, suggesting there is specificity of the interaction between SLDs and the Mus81 complex.

In summary, Esc2 interacts with the Mus81 complex via its SLDs. Furthermore, despite the sequence similarity between ySUMO and the SLDs, the Mus81 complex interacts specifically with the SLDs of Esc2.

Esc2 specifically stimulates the Mus81 complex activity

The interaction between Esc2 and the Mus81 complex, and Esc2's preferential binding to the substrates cleavable by the Mus81 complex (14,38), prompted us to further test the effect of Esc2 on the enzymatic activity of the Mus81 complex. To this end, we incubated increasing concentrations of Esc2 together with the Mus81 complex, which was present at a concentration to cleave about 10% of the substrate (Figure 4, lanes 2). Remarkably, Esc2 substantially stimulated the enzymatic activity of the Mus81 complex on all tested substrates (Figure 4). The stimulation was observable already at the lowest concentration of Esc2 tested (15.6 nM) (Figure 4A, lane 3). At this concentration, the stimulation was about 2-fold with the maximum stimulation (6-fold) observed at 250 nM Esc2 (Figure 4A, lane 7). Similar stimulation was also observed for other DNA substrates (Figure 4B and C). Thus, the presence of Esc2 together with

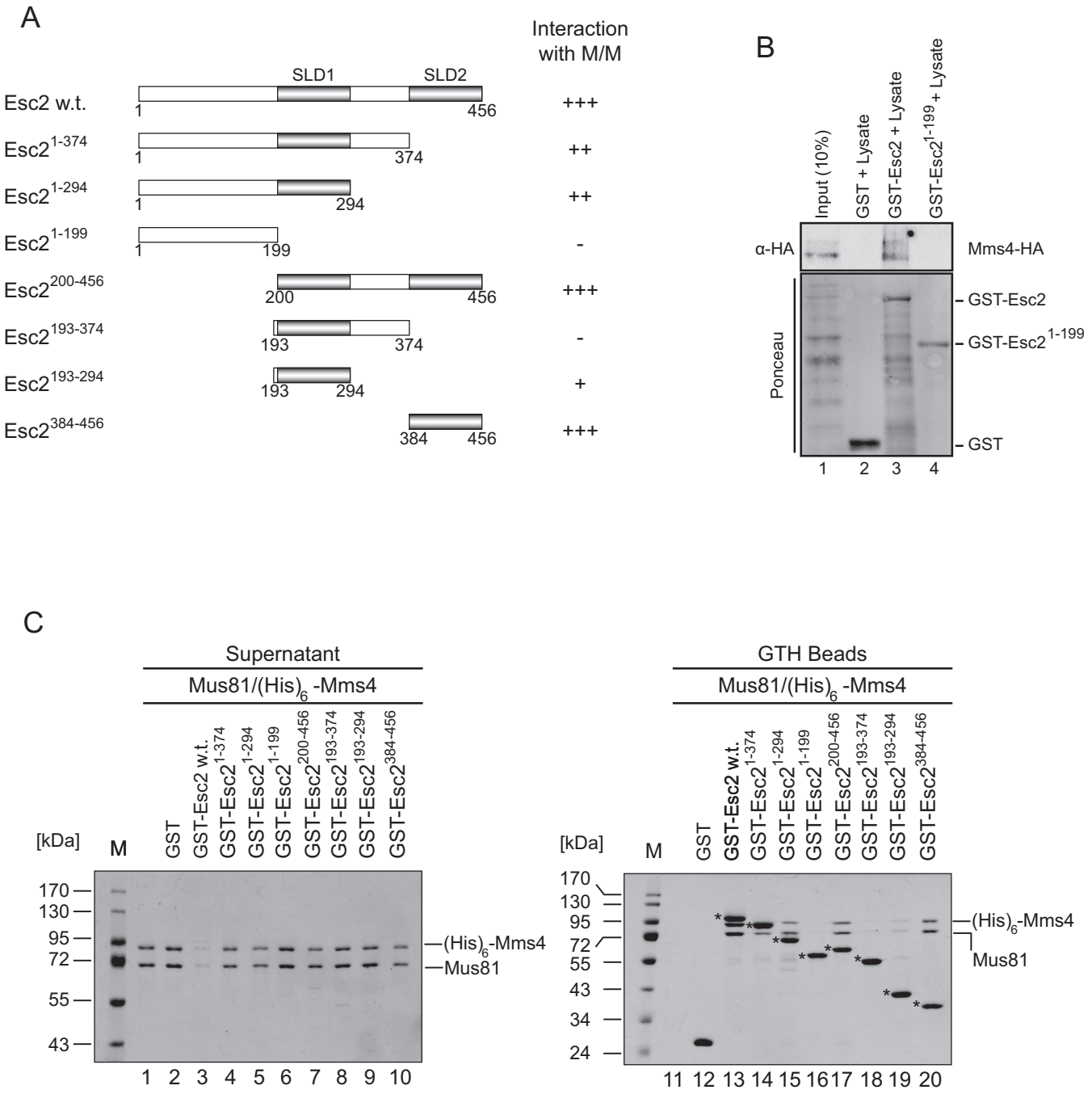

Figure 3. SUMO-like domains of Esc2 mediate the interaction between the Mus81 complex and Esc2. (**A**) Schematic representation of Esc2 fragments used in this study. (**B**) SUMO-like domains of Esc2 are required for the interaction between Esc2 and the Mus81 complex *in vivo*. The GST pull-down assay was performed as described before. Lane 1: 10% input, lane 2: GST incubated with total cell lysate, lane 3: GST-Esc2 incubated with total cell lysate and lane 4: GST-Esc2 1–198 incubated with total cell lysate. The reactions were analyzed by protein blotting using anti-HA antibodies (top panel) and Ponceau staining (bottom panel). (**C**) SUMO-like domains of Esc2 are required for the interaction between Esc2 and the Mus81 complex *in vitro*. The Mus81 complex (3 μg) was mixed with GST-tagged wild-type and various Esc2 truncations (3 μg each) in presence of glutathione beads, as indicated in the figure. After incubation, the beads were washed and treated with SDS to elute bound proteins. The supernatants with unbound proteins, and the SDS elution fractions were analyzed by SDS-PAGE and visualized by Coomassie Blue staining. Lanes 1 and 11 represent control experiments, where the Mus81 complex was incubated with glutathione beads alone. Position of Mus81 and $(His)_6$-Mms4 is indicated. * indicates position of the Esc2 truncations.

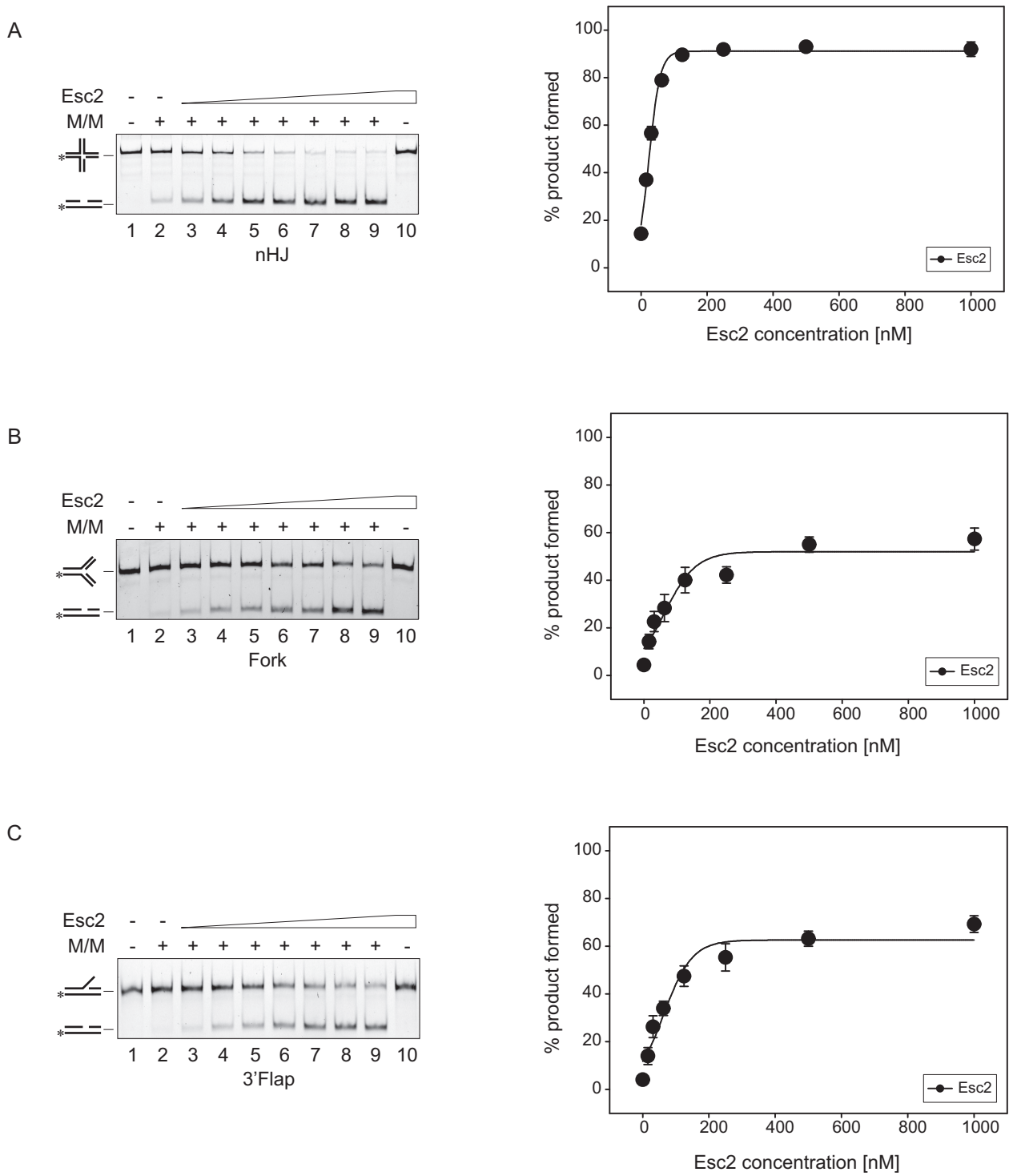

Figure 4. Esc2 stimulates the Mus81 complex activity on all substrates tested. Nuclease assays of the Mus81 complex (M/M) in the presence of Esc2. The Mus81 complex (0.05 nM) was incubated with increasing concentrations of Esc2 (16, 31, 63, 125, 250, 500 and 1000 nM) in the presence of nicked HJ (**A**), fork (**B**) and 3′flap substrate (**C**) (7 nM each), respectively. After incubation, the reaction mixtures were separated on native PAGE and analyzed. Quantification of the data shown in next to the gels. Error bars represent standard error from three independent experiments.

the Mus81 complex results in a dramatic stimulation of the Mus81 complex nuclease activity on various substrates, suggesting that these two proteins may cooperate in the resolution of SCJs, as well as other substrates of the Mus81 nuclease *in vivo*.

The stimulation of Mus81 activity by Esc2 is specific and requires both the DNA binding and the SLD domains of Esc2

Next, we tested the specificity of Esc2 towards the Mus81 complex. Therefore, we examined whether Rad27, a nuclease acting in Okazaki fragment maturation (39,40), Rad1-Rad10, another member of XPF/MUS81 family involved in nucleotide excision repair (41), and human MUS81–EME1 complex (42,43), are also stimulated by Esc2. Initially, we tested Esc2 interaction with these proteins using *in vitro* pull-down. We found that Esc2 did not interact with Rad27 (Supplementary Figure S5A) and interacted very poorly either with Rad1-Rad10 nuclease or with hMUS81–EME1 (Supplementary Figure S5B and C, respectively, compare with Figure 1A). Furthermore, we tested these enzymes in nuclease assays in the presence or absence of Esc2. Again, we used concentrations of Rad27, Rad1–Rad10 and hMUS81-EME1 at which these proteins cleaved 10–20% of their respective substrates (5′Flap, Y-form and nHJ, respectively). Addition of Esc2 did not affect enzymatic activity of either Rad27 or Rad1-Rad10 (Supplementary Figure S5D and S5F), suggesting that the stimulatory effect of Esc2 on the Mus81 complex is specific. Furthermore, we tested whether the stimulatory effect of Esc2 on the Mus81 complex is species-specific. Similarly, presence of Esc2 had no effect on the hMUS81-EME1 activity (Supplementary Figure S5E and S5F), confirming the species-specific stimulatory effect of Esc2 on the Mus81 complex. Additionally, we investigated whether Esc2 affects enzymatic activity of Yen1, a nuclease capable of resolving HJ that has been involved in metabolism of HJs emanating during HR (25,44,45). Initially, we studied genetic interactions between *ESC2* and *YEN1*. We tested sensitivity of single mutants (*Δesc2* and *Δyen1*) and a double mutant *Δesc2Δyen1* to MMS. *Δesc2 Δyen1* cells were as sensitive as sensitive to MMS as *Δesc2* at high concentrations of MMS (0.015%) and were more sensitive than *Δesc2* at lower concentrations of MMS (0.01%) (Supplementary Figure S6). This latter result resembles what has been reported for Δmus81 Δyen1 strains (46). This result further supports the notion that Esc2 stimulates the nuclease activity of the Mus81 complex specifically.

In order to map the Esc2 domain responsible for the stimulation of the Mus81 nuclease activity, we used the above-described truncated forms of Esc2 (Figure 5A). Incubation of $Esc2^{1\text{-}374}$ and $Esc2^{1–294}$ fragments with the Mus81 complex led to stimulation of the nuclease activity on the nHJ substrate comparable to that observed for wild-type Esc2 (Figure 5B). In contrast, $Esc2^{\Delta 154–198}$ showed significant decrease in the stimulation of the nuclease activity, and $Esc2^{1–199}$ and $Esc2^{200–456}$ did not stimulate the nuclease activity at all (Figure 5B, Supplementary Figure S8D and S8E), suggesting that both DNA binding and the Mus81 complex interaction domains are required for the observed stimulation. Thus, Esc2 stimulates the Mus81 complex in a nuclease- and species-specific manner and both the DNA binding domain and the domain mediating direct physical interaction between Esc2 and the Mus81 are required for this stimulation.

Esc2 cooperates with the Mus81 complex in resolution of SCJs molecules *in vivo*

Next, we wished to investigate the *in vivo* relevance of the observed stimulation of the Mus81 nuclease activity by Esc2. Therefore, we monitored the kinetics of Mus81-dependent resolution of SCJs molecules *in vivo*. We used an *sgs1Δ* genetic background to induce the dependence of their resolution on the Mus81 complex (9). Furthermore, we used a conditional Tc-*ESC2*-AID allele to overcome the synthetic sickness of *sgs1Δ esc2Δ* cells (Figure 6A) (30). The kinetics of SCJs resolution were followed for up to 6 h after the release from MMS by 2-D gel electrophoresis. As seen in the Figure 6B, in cells expressing Esc2, the signal representing SCJs started to decay already at 2 h post release from MMS and it eventually disappeared within 6 hours (upper panel). This contrasted to Esc2 depleted cells, which were delayed in resolving the SCJs, particularly at 3 and 4 h time-point, respectively (Figure 6B; compare upper and lower panel and the quantification in Figure 6C). The observed kinetics were similar to the kinetics exhibited by cells depleted for the Mus81 complex (Supplementary Figure S7A, B; and (9)), suggesting that Esc2 may be involved in Mus81-dependent resolution of SCJs. To further corroborate this finding, we tested genetic interaction of $esc2^{\Delta 154–198}$ allele (an Esc2 variant that binds DNA poorly, and hence fails to fully stimulate the Mus81-complex *in vitro*) with *Δsgs1*, the main factor responsible for SCJs dissolution. As it can be already seen from the tetrad analysis (Supplementary Figure S8B), double $esc2^{\Delta 154–198}$ *Δsgs1* cells show growth defect similar to *Δesc2 Δsgs1*, suggesting that binding of structured-DNA and full extent of the stimulation of the Mus81 complex is crucial function of Esc2 in the absence of *SGS1*. These results suggest that Esc2 plays a role in the late resolution of SCJs, which is crucially dependent on the Mus81 complex activity, also *in vivo*.

DISCUSSION

Replication across damaged templates is accompanied by the formation of SCJs that are toxic for chromosome segregation (5,9,25,47). If left unresolved, they represent a source of chromosome lesions and crossovers (48–50). The Mus81 complex has been implicated in the resolution of persistent SCJs in G2/M, in a parallel pathway to the STR complex, which represents the main mechanism for dissolution of these DNA structures from S to G2/M (9,10). Similarly to STR mutants, deletion of *ESC2* also results in SCJ accumulation in S phase (30,31), but the functional links between Esc2 and the other known resolvases (STR and the Mus81 complex) remained elusive.

In the present work, we tested cooperation between Esc2 and the Mus81 complex in the metabolism of intermediates emanating from the error-free DDT. We determined that Esc2 binds HJs, an *in vitro* proxy to the SCJs observed *in vivo* (47), with the highest affinity among all tested substrates. Moreover, we mapped the DNA binding domain,

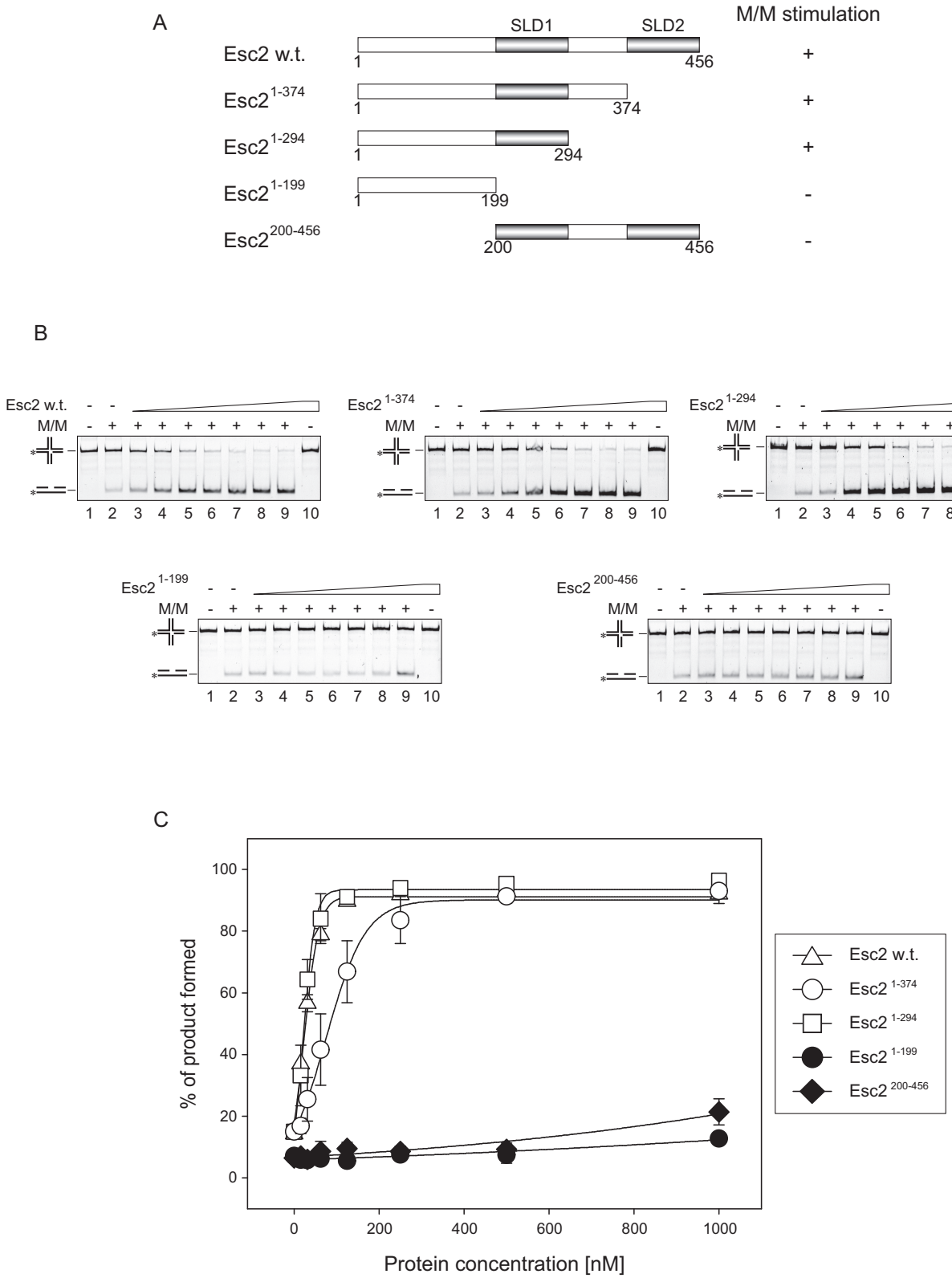

Figure 5. DNA binding and the interaction with the Mus81 complex are required for Esc2-mediated stimulation of the Mus81 complex. (**A**) Schematic representation of Esc2 fragments used in the assay. **B**) Nuclease assays of the Mus81 complex (M/M) in the presence of various Esc2 fragments. The Mus81 complex (0.05 nM) was incubated with increasing concentrations of the indicated Esc2 fragments (16, 31, 63, 125, 250, 500 and 1000 nM) in the presence of nicked Holliday junction (nHJ, 7 nM). After incubation, reactions were stopped by SDS/PK, and the reaction mixtures were separated on native PAGE and analyzed. (**C**) Quantification of the data shown in (**B**). Error bars represent standard error from three independent experiments.

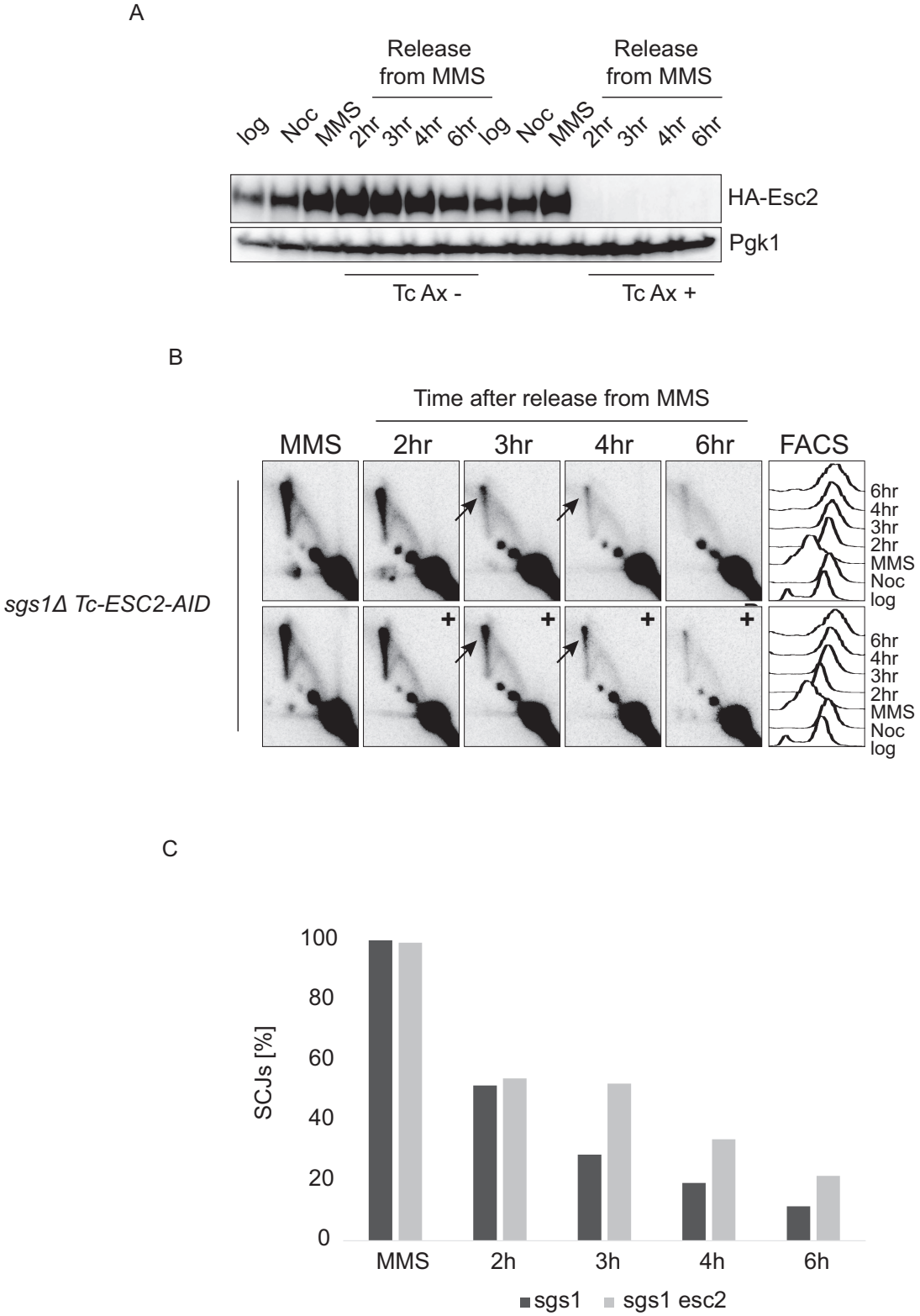

Figure 6. Esc2 and Mus81 cooperate in the resolution of SCJs *in vivo*. (**A**) Esc2 is effectively depleted upon addition of tetracycline (Tc) and auxin (Ax). G2/M synchronised *sgs1Δ Tc-ESC2-AID* cells were treated with MMS for 90 min (MMS), then released into YPD media in two identical sets of cultures, one set in the absence (labelled Tc Ax -) or presence of Tc and Ax (labelled with Tc Ax +). Samples were taken at indicated time-points. Presence of HA-tagged Esc2 upon addition of Tc and Ax was monitored by western blotting. Immunodetection of Pgk1 served as a loading control. (**B**) Esc2 promotes Mus81-dependent resolution of SCJs *in vivo*. The experiment was performed as described in (A). Samples were analysed by 2D gel electrophoresis and FACS. Replication intermediates were visualised using a radioactively labelled probe specific for *ARS305* in 2D gel electrophoresis. (**C**) Quantification of the data shown in (B). The signal representing the SCJs was quantified. The intensity of the signal corresponding to SCJs at the 0-hour time-point when the accumulation of X-molecules was at its highest was set as 100%.

showing it to be located in the region corresponding to AA 154–198. Importantly, our analysis of secondary structures in the Esc2 truncations by circular dichroism (CD) further supported this notion, as the CD spectrum of Esc2$^{1–199}$ resembles poly-l-proline-II type (PPII) helix. PPII helix was shown that it forms flexible blocks in folded protein structure and supports protein-protein or protein-nucleic acid interactions (51,52). Hence, the CD studies are in agreement with the notion that Esc2 protein harbors a DNA-binding domain. The direct binding of Esc2 to HJs potentially provides an explanation for the accumulation of SCJs in the *esc2Δ* cells. The roles of Esc2 in SCJ metabolism are, however, broader than the ones of the Mus81 complex, as differently to *esc2Δ*, *mus81Δ* mutants do not accumulate SCJs in S phase (9,10,30,31). It is, nonetheless, possible that the late effect of the Mus81 complex on resolving SCJs depends, in part, on Esc2. The preferential binding of Esc2 towards HJs *in vitro* is reminiscent of Rmi1, a structural component of the STR complex (53). Later, Rmi1 was shown to stimulate the decatenation of dHJs by Top3, and this activity required DNA binding property of Rmi1 (54). Therefore, we speculate that Esc2, similarly to Rmi1, can serve as adaptor protein to promote the activity the Mus81 complex at a subset of its substrates.

The ability of Esc2 to recognize recombination intermediates prompted us to test the interaction between Esc2 and Mus81 complex both *in vivo* and *in vitro*. Our results show that Esc2 interacts with the Mus81 complex throughout the cell cycle. This suggests that the cell cycle-dependent interplay of checkpoint- and CDK-dependent phosphorylation of Mms4 is not crucial for its interaction with Esc2. This notion was further substantiated by no observable change in the Esc2–Mus81 complex interaction when a phosphomimic variant of Mms4 (Mms4^{S56E}), resembling CDK-dependent activation of the Mus81 complex specifically in G2/M phase, was used (9,25,26). The results support the view that cell cycle-dependent phosphorylation-mediated activation of Mus81 and Esc2-mediated interaction with the Mus81 complex are not mutually exclusive. Furthermore, upon zeocin-induced DNA damage, Esc2 and the Mus81 complex co-localize in cells, corroborating our *in vitro* experiments. However, deletion of Esc2 has no effect on the ability of the Mus81 complex to form zeocin-induced foci, suggesting that Esc2 does not play a role in recruitment of the nuclease complex to damaged site.

Given the sequence and structural similarity between the Esc2 SUMO-like domains and the ySUMO (Supplementary Figure S3A and (29)), we studied whether ySUMO also interacts with the Mus81 complex. Strikingly, we observed no interaction between the Mus81 complex and ySUMO. A more detailed sequence comparison of the SLD2 and ySUMO revealed difference in two phenylalanine residues located in SLD2 domain responsible for the interaction between SUMO and SUMO-interacting motif (SIM) (F36, F37) (55,56), supporting the view that there is specificity of SLD2 interaction with the Mus81 complex. This result suggests the existence of mutually exclusive set of interacting partners and different roles for the SLD- and SUMO-mediated interactions. Since SUMOylation has recently been proposed to act as a 'molecular glue' (57,58), triggering transient and reversible association of proteins involved in the same pathway, we speculate that the SLD-mediated interactions may serve as scaffolds to form transient complexes at various, damage-specific locations and/or substrates. Similar behavior was recently reported for Srs2 and its interacting partners (59). Furthermore, a recent evidence suggest that the *Drosophila* orthologue of Esc2, *Dm*Rad60, promotes genome stability by delocalization of heterochromatic DSBs into nuclear periphery, may point in this direction (60). Moreover, the peculiar domain architecture of Esc2, with SUMO-like sequence being directly embedded in the protein sequence, would make it immune to deSUMOylation, thus allowing local accumulation of specific proteins or complexes.

The ability of Esc2 to specifically stimulate the *in vitro* Mus81 nuclease activity was further corroborated and strengthened by the role of Esc2 in promoting Mus81-dependent resolution of DDT intermediates *in vivo*. Esc2 may promote activity of the Mus81 complex in other *in vivo* contexts, including HR-mediated restart of collapsed replication forks, since Esc2 was shown to maintain the genome stability in multiple ways (32). The Mus81 complex and other nucleases involved in DNA replication and/or repair, including Rad27 and Rad1-Rad10, are stimulated and targeted by a diverse array of repair and replication proteins. Examples include PCNA and RFC-complex, which stimulate Rad27 (61–63) as well as Srs2 and Rad54 promoting the activity of the Mus81 complex (34,64,65). Mechanistically, these stimulatory factors interact with the particular nuclease, resulting in formation of a complex that cleaves the substrate more efficiently than the nuclease alone, pointing to a requirement for the specific interaction domain on the stimulating protein. However, the DNA binding of these stimulating proteins is, in general, dispensable for the stimulation. This is true for the Mus81 complex stimulation by Rad54 (34,64) or Srs2 (65). However, the Esc2-mediated activation of Mus81 complex differs from the pattern described above, as it requires both the protein-interaction domain as well as the DNA binding domain of Esc2 to stimulate the Mus81 complex arguing for a more complex mechanism of stimulation.

Based on our new and previously reported data, a possible scenario (Figure 7) in which Esc2 and the Mus81 complex may cooperate to promote genome stability. Esc2 may bind SCJs arising during error-free DDT, and thereby stimulate the Mus81 complex to resolve those structures. There are several pathways known to be involved in the processing of recombination intermediates. Mechanistically, they can be divided into two groups: (i) the dissolution mediated by the STR complex, which consists of convergent branch-migration coordinated with decatenation (66,67); and (ii) resolution mediated by, at present, four different nuclease complexes including: the Mus81 complex (9,14,25,26); Slx1-Slx4 (68); Yen1 (44); and MutLγ-Exo1 (69,70). In vivo, besides the STR complex (47), a contribution of the Mus81-Mms4 complex, likely in the context of the Slx4 scaffold has emerged (9,27). Additionally, the Mus81 complex is required for initiation of mitotic DNA synthesis upon mild replication stress in humans (24). Notably, single HJ-like substrates, which arise during recombination and fork-restart and are not substrates for the STR complex, need to be resolved before chromosome segregation (19).

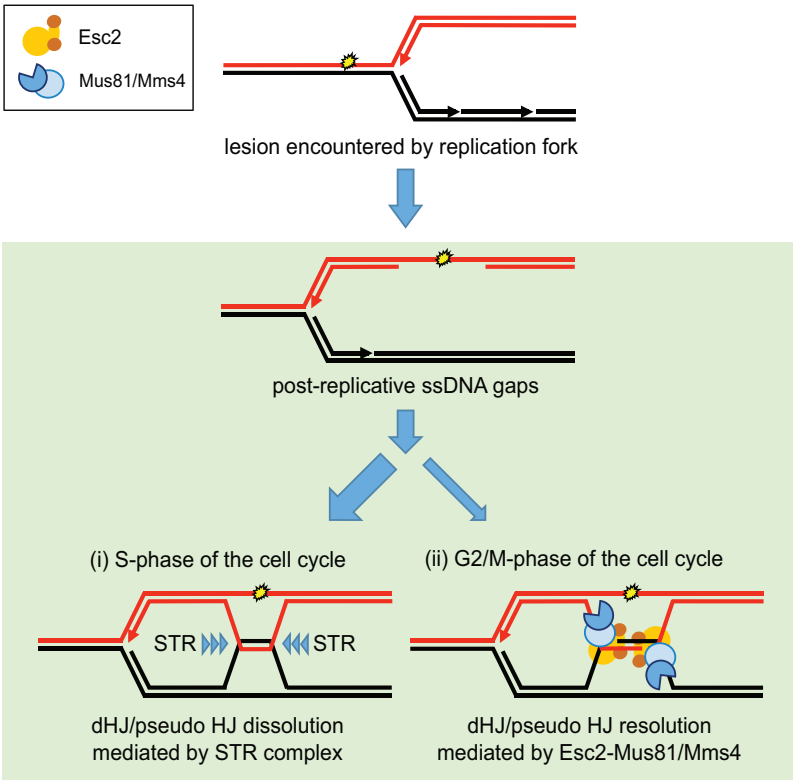

Figure 7. Model of the role of Esc2-Mus81 interaction in promoting genome stability. Hypothetical scenario by which Esc2 and the Mus81 complex may cooperate to promote genome stability is illustrated. Esc2 and the Mus81 complex may function during the metabolism of sister chromatid junctions (SCJs). Esc2 may specifically bind the 4-way intermediates (Holliday junctions or pseudo Holliday junctions), stimulating the activity of the Mus81 complex towards resolution.

The envisaged action of the Mus81 complex on such single HJ-like substrates, and its stimulation by Esc2, potentially explains the synthetic sickness between *sgs1Δ* mutants and either *esc2Δ* and *mus81Δ* (30). However, considering the synthetic sickness of *mus81Δ esc2Δ* double mutant (30,71), it is likely that Esc2 and the Mus81 complex act independently of each other in specific contexts related to either particular genomic locations (i.e. silent chromatin for Esc2) or specific recombination steps (i.e. early stages of the HR-mediated repair for the Mus81 complex). Future identification of conditional and separation-of-function alleles of *MUS81* or *ESC2* may provide new and exciting insights into their mode of action.

Recent works on the metabolism of HJs and HJ-like structures have yielded a comprehensive picture of the pathways involved in their resolution throughout the cell cycle (reviewed in (72)). However, the molecular mechanism and regulation of these pathways is still not clear. This work adds another piece into the complex mosaic of the ways by which various X-shaped intermediates arising during DNA metabolism are processed to maintain genomic stability.

SUPPLEMENTARY DATA

Supplementary Data are available at NAR Online.

ACKNOWLEDGEMENTS

We thank Zdenka Hašanová, Petra Matulová and Alexandra Sisáková for providing Rad1-Rad10, Rad27 and human MUS81-EME1 proteins, respectively. We thank Ondrej Beláň for help with drawing the model. We thank S. Brill, B. Shen, S. West for providing plasmids used to purify the proteins.

Author contribution: M.S. and L.K. conceived and designed the research. M.S. purified proteins, performed the *in vitro* experiments. M.P. purified a subset of proteins and performed experiments shown in Figure 3C and Supplementary Figure S3B. B. Stefanovie purified and characterized Esc2$^{\Delta 154\text{-}198}$ variant and performed experiments shown in Supplementary Figures S1 and S8. M.U., B. Szakal and D.B. established strains and performed experiments shown in Figures 2B-C, 3B, 6, Supplementary Figures S3, S6, S7, S8B. M.L. performed experiments shown in Figure 2D-F. M.S. and L.K. wrote the paper and all authors provided editorial assistance.

FUNDING

This project was supported by Czech Science Foundation [GACR 13-26629S and 207/12/2323]; LQ1605 from the National Program of Sustainability II (MEYS CR); Research Support Programme [GAMU – MUNI/M/1894/2014] to L.K., ERC [242928]; AIRC and Fondazione Telethon (to D.B.); M.S. was recipient of

SIPOD fellowship, co-funded by Marie-Curie Actions; The Danish Agency for Science, Technology and Innovation and the Villum Foundation provided support (to M.L.). Funding for open access charge: GACR [13-26629S].
Conflict of interest statement. None declared.

REFERENCES

1. Jackson,S.P. and Bartek,J. (2009) The DNA-damage response in human biology and disease. *Nature*, **461**, 1071–1078.
2. Branzei,D. (2011) Ubiquitin family modifications and template switching. *FEBS Lett.*, **585**, 2810–2817.
3. Ulrich,H.D. (2011) Timing and spacing of ubiquitin-dependent DNA damage bypass. *FEBS Lett.*, **585**, 2861–2867.
4. Zhang,H. and Lawrence,C.W. (2005) The error-free component of the RAD6/RAD18 DNA damage tolerance pathway of budding yeast employs sister-strand recombination. *Proc. Natl. Acad. Sci. U.S.A.*, **102**, 15954–15959.
5. Branzei,D., Vanoli,F. and Foiani,M. (2008) SUMOylation regulates Rad18-mediated template switch. *Nature*, **456**, 915–920.
6. Minca,E.C. and Kowalski,D. (2010) Multiple Rad5 activities mediate sister chromatid recombination to bypass DNA damage at stalled replication forks. *Mol. Cell*, **38**, 649–661.
7. Vanoli,F., Fumasoni,M., Szakal,B., Maloisel,L. and Branzei,D. (2010) Replication and recombination factors contributing to recombination-dependent bypass of DNA lesions by template switch. *PLoS Genet.*, **6**, e1001205.
8. Karras,G.I., Fumasoni,M., Sienski,G., Vanoli,F., Branzei,D. and Jentsch,S. (2012) Noncanonical role of the 9-1-1 clamp in the error-free DNA damage tolerance pathway. *Mol. Cell*, doi:10.1016/j.molcel.2012.11.016.
9. Szakal,B. and Branzei,D. (2013) Premature Cdk1/Cdc5/Mus81 pathway activation induces aberrant replication and deleterious crossover. *EMBO J.*, **32**, 1155–1167.
10. Ashton,T.M., Mankouri,H.W., Heidenblut,A., McHugh,P.J. and Hickson,I.D. (2011) Pathways for Holliday junction processing during homologous recombination in Saccharomyces cerevisiae. *Mol. Cell. Biol.*, **31**, 1921–1933.
11. Ciccia,A., Constantinou,A. and West,SC. (2003) Identification and characterization of the human Mus81-Eme1 endonuclease. *J. Biol. Chem.*, **278**, 25172–25178.
12. Whitby,M.C., Osman,F. and Dixon,J. (2003) Cleavage of model replication forks by fission yeast Mus81-Eme1 and budding yeast Mus81-Mms4. *J. Biol. Chem.*, **278**, 6928–6935.
13. Ogrunc,M. and Sancar,A. (2003) Identification and characterization of human MUS81-MMS4 structure-specific endonuclease. *J. Biol. Chem.*, **278**, 21715–21720.
14. Fricke,W.M., Bastin-Shanower,S.A. and Brill,S.J. (2005) Substrate specificity of the Saccharomyces cerevisiae Mus81–Mms4 endonuclease. *DNA Repair (Amst.)*, **4**, 243–251.
15. Ehmsen,K.T. and Heyer,W.D. (2008) Saccharomyces cerevisiae Mus81-Mms4 is a catalytic, DNA structure-selective endonuclease. *Nucleic Acids Res.*, **36**, 2182–2195.
16. Interthal,H. and Heyer,W.D. (2000) MUS81 encodes a novel Helix-hairpin-Helix protein involved in the response to UV- and methylation-induced DNA damage in Saccharomyces cerevisiae. *Mol. Gen. Genet. MGG*, **263**, 812–827.
17. Osman,F. and Whitby,M. (2007) Exploring the roles of Mus81-Eme1/Mms4 at perturbed replication forks. *DNA Repair (Amst.)*, **6**, 1004–1017.
18. Regairaz,M., Zhang,Y.-W., Fu,H., Agama,K.K., Tata,N., Agrawal,S., Aladjem,M.I. and Pommier,Y. (2011) Mus81-mediated DNA cleavage resolves replication forks stalled by topoisomerase I–DNA complexes. *J. Cell Biol.*, **195**, 739–749.
19. Mayle,R., Campbell,I.M., Beck,C.R., Yu,Y., Wilson,M., Shaw,C.A., Bjergbaek,L., Lupski,J.R. and Ira,G. (2015) Mus81 and converging forks limit the mutagenicity of replication fork breakage. *Science*, **349**, 742–747.
20. Oh,S.D., Lao,J.P., Hwang,P.Y.-H., Taylor,A.F., Smith,G.R. and Hunter,N. (2008) BLM ortholog, Sgs1, prevents aberrant crossing-over by suppressing formation of multichromatid joint molecules. *Cell*, **130**, 259–272.
21. Jessop,L. and Lichten,M. (2008) Mus81/Mms4 endonuclease and Sgs1 helicase collaborate to ensure proper recombination intermediate metabolism during meiosis. *Mol. Cell*, **31**, 313–323.
22. Ying,S., Minocherhomji,S., Chan,K.L., Palmai-Pallag,T., Chu,W., Wass,T., Mankouri,H.W., Liu,Y. and Hickson,I.D. (2013) MUS81 promotes common fragile site expression. *Nat. Cell Biol.*, **15**, 1001–1007.
23. Naim,V., Wilhelm,T., Debatisse,M. and Rosselli,F. (2013) ERCC1 and MUS81–EME1 promote sister chromatid separation by processing late replication intermediates at common fragile sites during mitosis. *Nat. Cell Biol.*, **15**, 1008–1015.
24. Minocherhomji,S., Ying,S., Bjerregaard,V.A., Bursomanno,S., Aleliunaite,A., Wu,W., Mankouri,H.W., Shen,H., Liu,Y. and Hickson,I.D. (2015) Replication stress activates DNA repair synthesis in mitosis. *Nature*, **528**, 286–290.
25. Matos,J., Blanco,M.G., Maslen,S., Skehel,J.M. and West,S.C. (2011) Regulatory control of the resolution of DNA recombination intermediates during meiosis and mitosis. *Cell*, **147**, 158–172.
26. Gallo-Fernández,M., Saugar,I., Ortiz-Bazán,M.Á., Vázquez,M.V. and Tercero,J.A. (2012) Cell cycle-dependent regulation of the nuclease activity of Mus81–Eme1/Mms4. *Nucleic Acids Res.*, **40**, 8325–8335.
27. Gritenaite,D., Princz,L.N., Szakal,B., Bantele,S.C.S., Wendeler,L., Schilbach,S., Habermann,B.H., Matos,J., Lisby,M., Branzei,D. *et al.* (2014) A cell cycle-regulated Slx4–Dpb11 complex promotes the resolution of DNA repair intermediates linked to stalled replication. *Genes Dev.*, **28**, 1604–1619.
28. Dhillon,N. and Kamakaka,R.T. (2000) A Histone Variant, Htz1p, and a Sir1p-like Protein, Esc2p, Mediate Silencing at HMR. *Mol. Cell*, **6**, 769–780.
29. Novatchkova,M., Bachmair,A., Eisenhaber,B. and Eisenhaber,F. (2005) Proteins with two SUMO/like domains in chromatin/associated complexes: The RENi (Rad60/Esc2/NIP45) family. *BMC Bioinformatics*, **6**, 22.
30. Sollier,J., Driscoll,R., Castellucci,F., Foiani,M., Jackson,S.P. and Branzei,D. (2009) The Saccharomyces cerevisiae Esc2 and Smc5-6 Proteins Promote Sister Chromatid Junction-mediated Intra-S Repair. *Mol. Biol. Cell*, **20**, 1671–1682.
31. Mankouri,H.W., Ngo,H.-P. and Hickson,I.D. (2009) Esc2 and Sgs1 act in functionally distinct branches of the homologous recombination repair pathway in Saccharomyces cerevisiae. *Mol. Biol. Cell*, **20**, 1683–1694.
32. Urulangodi,M., Sebesta,M., Menolfi,D., Szakal,B., Sollier,J., Sisakova,A., Krejci,L. and Branzei,D. (2015) Local regulation of the Srs2 helicase by the SUMO-like domain protein Esc2 promotes recombination at sites of stalled replication. *Genes Dev.*, **29**, 2067–2080.
33. Thomas,B.J. and Rothstein,R. (1989) Elevated recombination rates in transcriptionally active DNA. *Cell*, **56**, 619–630.
34. Matulova,P., Marini,V., Burgess,R.C., Sisakova,A., Kwon,Y., Rothstein,R., Sung,P. and Krejci,L. (2009) Cooperativity of Mus81·Mms4 with Rad54 in the resolution of recombination and replication intermediates. *J. Biol. Chem.*, **284**, 7733–7745.
35. Silva,S., Gallina,I., Eckert-Boulet,N. and Lisby,M. (2012) Live cell microscopy of DNA damage response in Saccharomyces cerevisiae. *Methods Mol Biol.*, **920**, 433–443.
36. Orm,M., Cubitt,A.B., Kallio,K., Gross,L.A., Tsien,R.Y. and Remington,S.J. (1996) Crystal structure of the Aequorea victoria green fluorescent protein. *Science*, **273**, 1392–1395.
37. Goedhart,J., von Stetten,D., Noirclerc-Savoye,M., Lelimousin,M., Joosen,L., Hink,M.A., van Weeren,L., Gadella,T.W.J. and Royant,A. (2012) Structure-guided evolution of cyan fluorescent proteins towards a quantum yield of 93%. *Nat. Commun.*, **3**, 751.
38. Bartosova,Z. and Krejci,L. (2014) Nucleases in homologous recombination as targets for cancer therapy. *FEBS Lett.*, **588**, 2446–2456.
39. Ayyagari,R., Gomes,X.V., Gordenin,D.A. and Burgers,P.M.J. (2003) Okazaki fragment maturation in yeast: I. Distribution of functions between FEN1 and DNA2. *J. Biol. Chem.*, **278**, 1618–1625.
40. Kao,H.I., Henricksen,L.A., Liu,Y. and Bambara,R.A. (2002) Cleavage specificity of Saccharomyces cerevisiae flap endonuclease 1 suggests a double-flap structure as the cellular substrate. *J. Biol. Chem.*, **277**, 14379–14389.

41. Tomkinson,A.E., Bardwell,A.J., Bardwell,L., Tappe,N.J. and Friedberg,E.C. (1993) Yeast DNA repair and recombination proteins Rad1 and Rad10 constitute a single-stranded-DNA endonuclease. *Nature*, **362**, 860–862.
42. Chen,X.-B., Melchionna,R., Denis,C.-M., Gaillard,P.-H.L., Blasina,A., Van de Weyer,I., Boddy,M.N., Russell,P., Vialard,J. and McGowan,C.H. (2001) Human Mus81-associated endonuclease cleaves Holliday junctions in vitro. *Mol. Cell*, **8**, 1117–1127.
43. Boddy,M.N., Gaillard,P.-H.L., McDonald,W.H., Shanahan,P., Yates,J.R. and Russell,P. (2001) Mus81-Eme1 are essential components of a Holliday junction resolvase. *Cell*, **107**, 537–548.
44. Ip,S.C.Y., Rass,U., Blanco,M.G., Flynn,H.R., Skehel,J.M. and West,S.C. (2008) Identification of Holliday junction resolvases from humans and yeast. *Nature*, **456**, 357–361.
45. Ho,C.K., Mazón,G., Lam,A.F. and Symington,L.S. (2010) Mus81 and Yen1 promote reciprocal exchange during mitotic recombination to maintain genome integrity in budding yeast. *Mol. Cell*, **40**, 988–1000.
46. Blanco,M.G., Matos,J., Rass,U., Ip,S.C.Y. and West,S.C. (2010) Functional overlap between the structure-specific nucleases Yen1 and Mus81-Mms4 for DNA-damage repair in S. cerevisiae. *DNA Repair (Amst.)*, **9**, 394–402.
47. Giannattasio,M., Zwicky,K., Follonier,C., Foiani,M., Lopes,M. and Branzei,D. (2014) Visualization of recombination-mediated damage bypass by template switching. *Nat. Struct. Mol. Biol.*, doi:10.1038/nsmb.2888.
48. Gangloff,S., Fabre,F. and Soustelle,C. (2000) Homologous recombination is responsible for cell death in the absence of the Sgs1 and Srs2 helicases. *Nat. Genet.*, **25**, 192–194.
49. Krejci,L., Altmannova,V., Spirek,M. and Zhao,X. (2012) Homologous recombination and its regulation. *Nucleic Acids Res.*, **40**, 5795–5818.
50. Branzei,D. and Foiani,M. (2010) Maintaining genome stability at the replication fork. *Nat Rev Mol Cell Biol.*, **11**, 208–219.
51. Hicks,J.M. and Hsu,V.L. (2004) The extended left-handed helix: a simple nucleic acid-binding motif. *Proteins*, **55**, 330–338.
52. Siligardi,G. and Drake,A.F. (1995) The importance of extended conformations and, in particular, the PII conformation for the molecular recognition of peptides. *Biopolymers*, **37**, 281–292.
53. Chen,C.-F. and Brill,S.J. (2007) Binding and activation of DNA topoisomerase III by the Rmi1 subunit. *J. Biol. Chem.*, **282**, 28971–28979.
54. Cejka,P., Plank,J.L., Bachrati,C.Z., Hickson,I.D. and Kowalczykowski,S.C. (2010) Rmi1 stimulates decatenation of double Holliday junctions during dissolution by Sgs1–Top3. *Nat. Struct. Mol. Biol.*, **17**, 1377–1382.
55. Bergink,S., Ammon,T., Kern,M., Schermelleh,L., Leonhardt,H. and Jentsch,S. (2013) Role of Cdc48/p97 as a SUMO-targeted segregase curbing Rad51–Rad52 interaction. *Nat Cell Biol.*, **15**, 526–532.
56. Song,J., Zhang,Z., Hu,W. and Chen,Y. (2005) Small ubiquitin-like modifier (SUMO) recognition of a SUMO binding motif: a reversal of the bound orientation. *J. Biol. Chem.*, **280**, 40122–40129.
57. Psakhye,I. and Jentsch,S. Protein group modification and synergy in the SUMO pathway as exemplified in DNA repair. *Cell*, **151**, 807–820.
58. Jentsch,S. and Psakhye,I. (2013) Control of nuclear activities by substrate-selective and protein-group SUMOylation. *Annu. Rev. Genet.*, **47**, 167–186.
59. Kolesar,P., Altmannova,V., Silva,S., Lisby,M. and Krejci,L. (2016) Pro-recombination role of Srs2 protein requires SUMO (small ubiquitin-like modifier) but Is independent of PCNA (proliferating cell nuclear antigen) interaction. *J. Biol. Chem.*, **291**, 7594–7607.
60. Ryu,T., Spatola,B., Delabaere,L., Bowlin,K., Hopp,H., Kunitake,R., Karpen,G.H. and Chiolo,I. (2015) Heterochromatic breaks move to the nuclear periphery to continue recombinational repair. *Nat. Cell Biol.*, **17**, 1401–1411.
61. Gomes,X.V. and Burgers,P.M.J. (2000) Two modes of FEN1 binding to PCNA regulated by DNA. *EMBO J.*, **19**, 3811–3821.
62. Tom,S., Henricksen,L.A. and Bambara,R.A. (2000) Mechanism whereby proliferating cell nuclear antigen stimulates flap endonuclease 1. *J. Biol. Chem.*, **275**, 10498–10505.
63. Cho,I.-T., Kim,D.-H., Kang,Y.-H., Lee,C.-H., Amangyelid,T., Nguyen,T.A., Hurwitz,J. and Seo,Y.-S. (2009) Human replication factor C stimulates flap endonuclease 1. *J. Biol. Chem.*, **284**, 10387–10399.
64. Mazina,O.M. and Mazin,A.V. (2008) Human Rad54 protein stimulates human Mus81-Eme1 endonuclease. *Proc. Natl. Acad. Sci. U.S.A.*, **105**, 18249–18254.
65. Chavdarova,M., Marini,V., Sisakova,A., Sedlackova,H., Vigasova,D., Brill,S.J., Lisby,M. and Krejci,L. (2015) Srs2 promotes Mus81–Mms4-mediated resolution of recombination intermediates. *Nucleic Acids Res.*, **43**, 3626–3642.
66. Wu,L. and Hickson,I.D. (2003) The Bloom's syndrome helicase suppresses crossing over during homologous recombination. *Nat. Cell Biol.*, **426**, 870–874.
67. Cejka,P., Plank,J.L., Dombrowski,C.C. and Kowalczykowski,S.C. (2012) Decatenation of DNA by the S. cerevisiae Sgs1-Top3-Rmi1 and RPA complex: a mechanism for disentangling chromosomes. *Mol. Cell*, **47**, 886–896.
68. Fricke,W.M. and Brill,S.J. (2003) Slx1—Slx4 is a second structure-specific endonuclease functionally redundant with Sgs1—Top3. *Genes Dev.*, **17**, 1768–1778.
69. Zakharyevich,K., Tang,S., Ma,Y. and Hunter,N. (2012) Delineation of joint molecule resolution pathways in meiosis identifies a crossover-specific resolvase. *Cell*, **149**, 334–347.
70. Ranjha,L., Anand,R. and Cejka,P. (2014) The Saccharomyces cerevisiae Mlh1-Mlh3 heterodimer Is an endonuclease that preferentially binds to Holliday junctions. *J. Biol. Chem.*, **289**, 5674–5686.
71. Bellaoui,M., Chang M., Ou J., Xu H., Boone C., Brown G.W. (2003) Elg1 forms an alternative RFC complex important for DNA replication and genome integrity. *EMBO J.*, **22**, 4304–4313.
72. West,S.C., Blanco,M.G., Chan,Y.W., Matos,J., Sarbajna,S. and Wyatt,H.D.M. (2015) Resolution of Recombination Intermediates: Mechanisms and Regulation. *Cold Spring Harb. Symp. Quant. Biol.* , **80**, 103–109.